CityU Scholars

Molecular doping of blue phosphorene
A first-principles investigation

Sun, Minglei; Tang, Wencheng; Li, Song; Chou, Jyh-Pin; Hu, Alice; Schwingenschlögl, Udo

Document Version:
Final Published version, also known as Publisher's PDF, Publisher's Final version or Version of Record

Publication record in CityU Scholars:
Go to record

PAPER • OPEN ACCESS

Molecular doping of blue phosphorene: a first-principles investigation

View the article online for updates and enhancements.

Molecular doping of blue phosphorene: a first-principles investigation

Minglei Sun[1] , **Wencheng Tang**[2] , **Song Li**[3] , **Jyh-Pin Chou**[3] , **Alice Hu**[3]
and Udo Schwingenschlögl[1]

[1] Physical Science and Engineering Division (PSE), King Abdullah University of Science and Technology
(KAUST), Thuwal 23955-6900, Saudi Arabia
[2] School of Mechanical Engineering, Southeast University, Nanjing, Jiangsu 211189,
People's Republic of China
[3] Department of Mechanical Engineering, City University of Hong Kong, Kowloon 999077,
People's Republic of China

E-mail: jpchou@cityu.edu.hk and udo.schwingenschlogl@kaust.edu.sa

CrossMark

Abstract

Using first-principles calculations, we show that p-doped blue phosphorene can be
obtained by molecular doping with 2,3,5,6-tetrafluoro-7,7,8,8-tetracyanoquinodimethane
(F_4-TCNQ) and 1,3,4,5,7,8-hexafluorotetracyanonaphthoquinodimethane (F_6-TNAP),
whereas n-doped blue phosphorene can be realized by doping with tetrathiafulvalene (TTF)
and cyclooctadecanonaene (CCO). Moreover, the doping gap can be effectively modulated in
each case by applying an external perpendicular electric field. The optical absorption of blue
phosphorene can be considerably enhanced in a broad spectral range through the adsorption
of CCO, F_4-TCNQ, and F_6-TNAP molecules, suggesting potential of the doped materials in
the field of renewable energy.

Keywords: molecular doping, blue phospherene, doping gap, absorption, first-principles

S Supplementary material for this article is available online

(Some figures may appear in colour only in the online journal)

Introduction

Blue phosphorene (BlueP), a monolayer of phosphorus atoms
with buckled honeycomb structure, attracts much attention
because it combines fascinating features [1]. It is an intrinsic
semiconductor with a sizable bandgap in excess of 2 eV [1, 2],
which can be modulated by applying an electric field [3],
stacking effects [4, 5], functionalization [6–8], doping [9–11],
and formation of heterostructures [12–14]. Its mobility is as
high as 10^3 cm^2 V^{-1} s^{-1} [15], and the thermoelectric figure of
merit reaches values of 1.2 (p-doping) and 0.7 (n-doping)
already at room temperature [16]. BlueP has potential in
important applications such as nanoelectronic devices [17],
gas sensors [18, 19], lithium-ion batteries [20, 21], and pho-
tocatalysts [22–24]. It can be readily synthesized by epitaxial
growth on Au(1 1 1) [25–27] and GaN(0 0 1) [28] substrates.
Despite the promises of BlueP as two-dimensional (2D) semi-
conducting material, however, an effective approach to tune
its properties is necessary to facilitate future utilization.

Molecular doping of 2D materials was addressed in the
literature for graphene [29–44], MoS$_2$ [45–54], black phos-
phorene [55–59], arsenene [60, 61], and antimonene [62].
Concerning the effect of molecular doping on the electronic
properties, it was shown, for instance, that a bandgap can be
opened in graphene, which enables application in devices
such as field-effect transistors [32]. Adsorption of deca-
methylcobaltocene and 3,6-difluoro-2,5,7,7,8,8-hexacyano-
quinodimethane molecules on bilayer graphene was studied in
[36], achieving a bandgap of up to 0.15 eV. Molecular doping
is also a method to control the carrier type and amount in 2D
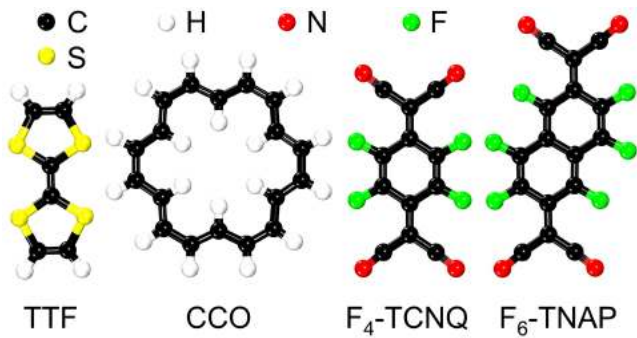
Figure 1. Top views of the atomic structures of TTF, CCO, F$_4$-TCNQ, and F$_6$-TNAP.

Table 1. Adsorption energy (E_{ad}), adsorption height (h), electron transfer (ΔQ), and injected carrier concentration (n; ΔQ per area).

	Adsorption site	E_{ad} (eV)	h (Å)	ΔQ (e)	n (10^{12} e cm^{-2})
BlueP–TTF	6	0.87	3.08	−0.11	3.3
BlueP–CCO	6	1.12	3.50	−0.04	1.2
BlueP–F$_4$-TCNQ	2	0.87	3.51	0.12	3.6
BlueP–F$_6$-TNAP	2, 6	1.11	3.37, 3.43	0.16	4.8

materials without perturbing the band structure (in contrast to traditional atomic doping) [37, 54, 56]. While monolayer graphene grown by ambient-pressure chemical vapor deposition shows p-type characteristics, transition to n-type characteristics can be realized by adsorption of piperidine, making it possible to form a graphene-based p-n junction [42]. Molecular doping can also be used to tune the optical properties of 2D materials. For instance, the photoluminescence intensity of monolayer MoS$_2$ is drastically enhanced by adsorption of 2,3,5,6-tetrafluoro-7,7,8,8-tetracyanoquinodimethane (F$_4$-TCNQ) or 7,7,8,8-tetracyanoquinodimethane (TCNQ) [45]. It can be enhanced by a factor of nine by doping with salicylic acid molecules [52]. While these investigations show that molecular doping is a very powerful approach to tune 2D materials and broaden their range of applications, the technique was not applied to BlueP so far.

In the present work, we therefore explore the effects of molecular doping on BlueP, using first-principles calculations. In addition, application of an external electric field is considered as a tool to modify the electronic properties. Four organic molecules (atomic structures illustrated in figure 1, see also figure S1 in the supporting information (stacks.iop.org/JPhysCM/32/055501/mmedia)) are investigated: tetrathiafulvalene (TTF) and cyclooctadecanonaene (CCO) as examples of electron donors (low ionization potentials of 6.83 and 7.23 eV, respectively [63, 64]), and F$_4$-TCNQ and 1,3,4,5,7,8-hexafluorotetracyanonaphthoquinodimethane (F$_6$-TNAP) as examples of electron acceptors (high electron affinities of 5.24 and 5.37 eV, respectively [65, 66]). We will demonstrate that adsorption of these molecules can yield p- and n-doping without breaking the 2D structure of BlueP. In addition, the ability to absorb sun light can be enhanced significantly, which is critical for the application of BlueP-based materials in energy harvesting.

Computational details

First-principles calculations are performed using the Vienna ab-initio simulation package based on plane-wave density functional theory and the projector-augmented wave method [67]. The energy cutoff of the plane-wave expansion is set to 450 eV and the exchange-correlation functional is treated in the generalized gradient approximation (Perdew–Burke–Ernzerhof
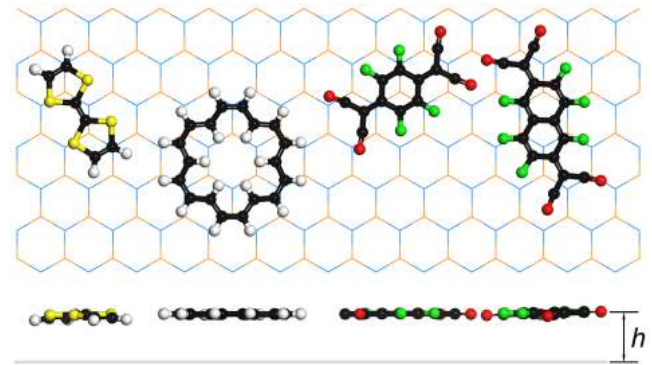

Figure 2. Top (upper panel) and side (lower panel) views of the favorable adsorption configurations of TTF, CCO, F$_4$-TCNQ, and F$_6$-TNAP molecules on BlueP. The orange and blue sticks represent upper and lower P atoms, respectively. The white, black, red, green, and yellow spheres represent H, C, N, F, and S atoms, respectively.

form). To describe the long-range interaction between BlueP and organic molecules, the vdW-D3 correction of Grimme is used [68]. The optB86b-vdW functional [69] is found to result in unreasonably large adsorption heights. A large $6 \times 6 \times 1$ supercell is adopted with a vacuum region thicker than 15 Å to eliminate artificial interaction between periodic images. One molecule is added to the supercell, which corresponds to an areal density of 3×10^{13} cm^{-2}. We can neglect substrate effects, because the binding energy between BlueP and the usual substrate, Au(1 1 1), is only 0.11 eV/atom [70]. Brillouin zone sampling on a Monkhorst-Pack $3 \times 3 \times 1$ k-mesh provides good convergence. In the structure optimization the atomic coordinates are relaxed until the Hellmann–Feynman forces are reduced to 0.01 eV Å^{-1}. Absorption spectra are calculated using the Heyd–Scuseria–Ernzerhof (HSE06) hybrid functional [71]. The imaginary part of the dielectric tensor is obtained by neglecting local field effects and approximating the macroscopic dielectric function by the head of the microscopic dielectric matrix [72]. The real part of the dielectric tensor then results from Kramers–Kronig transformation.

Results and discussion

We obtain for pristine BlueP an optimized lattice constant of 3.277 Å. Previously, Zhu *et al* [1] predicted a lattice constant of 3.33 Å, while Bao *et al* [20] obtained a value of 3.29 Å. Thus, our calculated lattice constant is in satisfactory agreement with previous results, demonstrating reliability of the methods used in the present work. We determine the
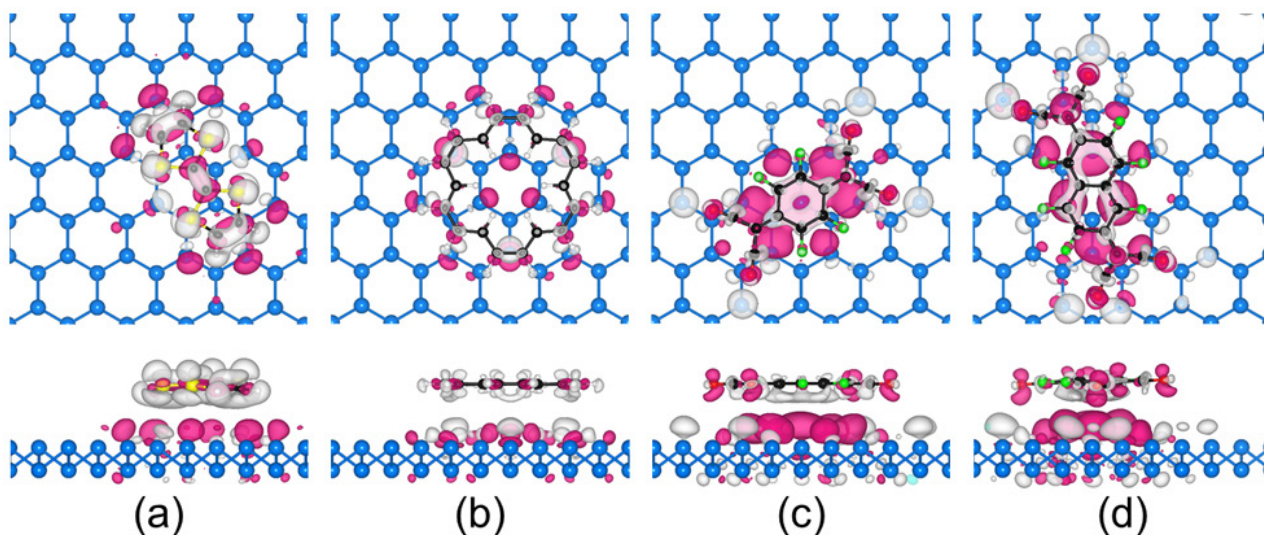
Figure 3. Top (upper panels) and side (lower panels) views of charge density difference isosurfaces (isovalue: 0.0003 e Å^{-3}) for (a) TTF–BlueP, (b) CCO–BlueP, (c) F_4-TCNQ–BlueP, and (d) F_6-TNAP–BlueP. The white, black, red, green, blue, and yellow spheres represent H, C, N, F, P, and S atoms, respectively. Pink color denotes electron accumulation and gray color electron depletion.
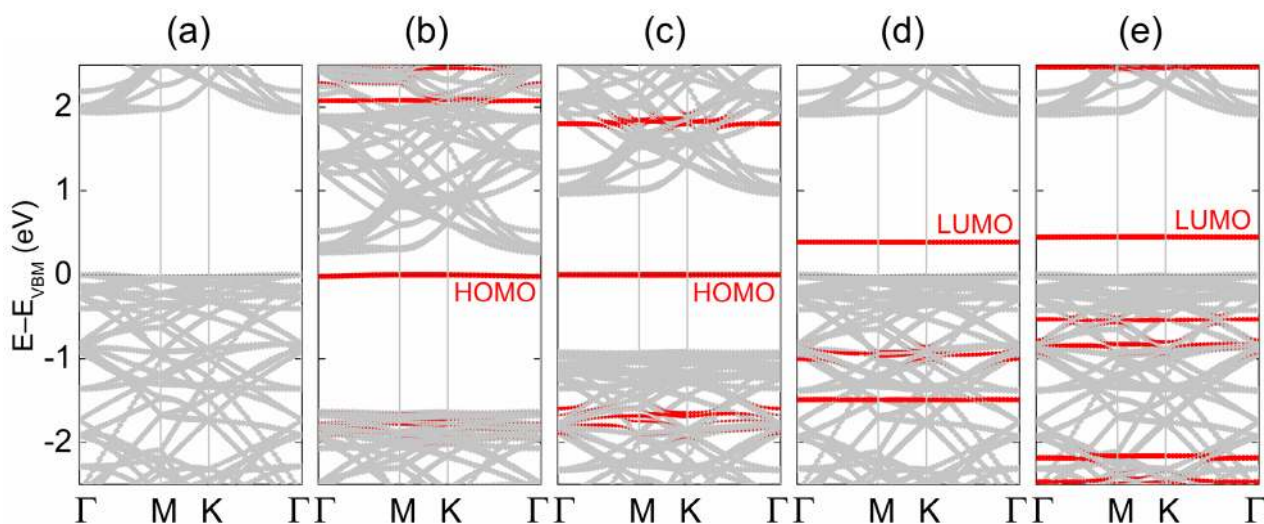

Figure 4. Projected band structures of (a) pristine BlueP, (b) TTF–BlueP, (c) CCO–BlueP, (d) BlueP–F_4-TCNQ, and (e) F_6-TNAP–BlueP. Red color highlights the contributions of the molecules.

favorable adsorption configuration for each molecule (table 1, figure 2) by calculating the adsorption energy $E_{ad} = E_{mol}$ $_{ecule} + E_{BlueP} − E_{BlueP+molecule}$, where $E_{molecule}$, E_{BlueP}, and $E_{BlueP+molecule}$ are the energies of the molecule, pristine BlueP, and BlueP with adsorbed molecule, respectively. For each molecule, several high-symmetry adsorption sites are considered (figure S2 in the supporting information). The TTF molecule favors alignment parallel to the zigzag direction of BlueP with $E_{ad} = 0.87$ eV and adsorption height $h = 3.08$ Å, the electron-abundant C_3S_2 rings located above P atoms. The CCO molecule favors a high symmetry configuration with space group C_{3v} ($E_{ad} = 1.12$ eV, $h = 3.50$ Å). The aromatic ring of the F_4-TCNQ molecule is located directly on top of a P atom to maximize the overlap between its delocalized π electrons and the p electrons of the P atom. In addition, two cyano groups cross the P–P

bonds, increasing the electron transfer and binding strength ($E_{ad} = 0.87$ eV and $h = 3.51$ Å). Finally, for the F_6-TNAP molecule there exist two adsorption sites with $E_{ad} = 1.11$ eV (2 and 6 in figure S1(d) with $h = 3.37$ and 3.43 Å, respectively). We choose the configuration presented in figure 2 for the following calculations.

Charge transfer in the molecule-doped materials may alter the transport and optical performance of BlueP, as revealed for the F_4-TCNQ/MoS_2 interface in an earlier study [45]. To investigate this question, figure 3 shows the charge density difference isosurfaces obtained for BlueP with adsorbed TTF, CCO, F_4-TCNQ, and F_6-TNAP molecules. The pink regions denote accumulation of electrons and the gray regions denote depletion of electrons. In the cases of TTF–BlueP and CCO–BlueP (figures 3(a) and (b)) electrons are transferred from the highest occupied molecular orbital (HOMO) to BlueP
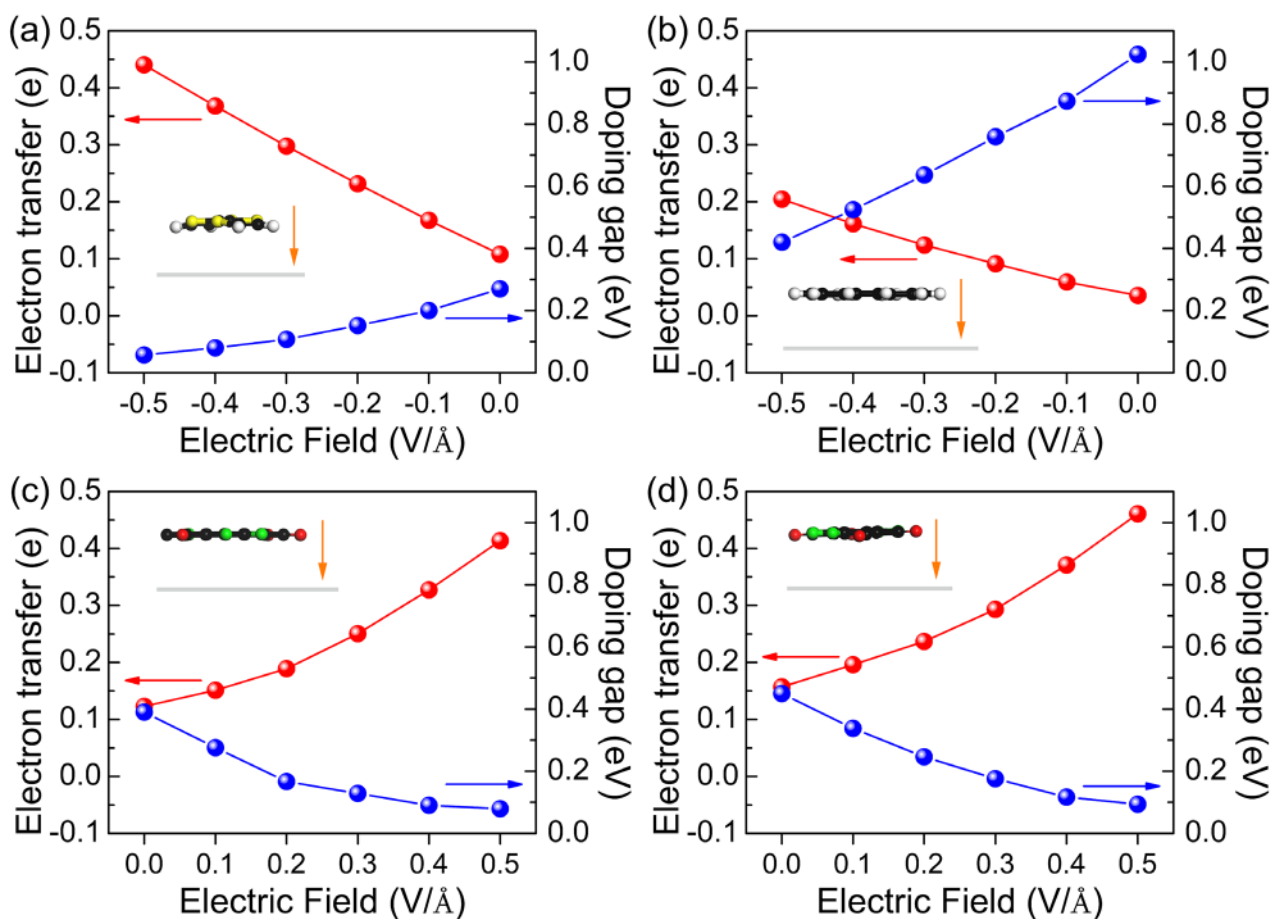
Figure 5. Doping gaps and electron transfer in (a) TTF–BlueP, (b) CCO–BlueP, (c) F_4-TCNQ–BlueP, and (d) F_6-TNAP–BlueP as functions of the electric field. The insets show the structure under an electric field of strength ± 0.5 V Å^{-1} and the orange arrows indicate the positive direction of this field.
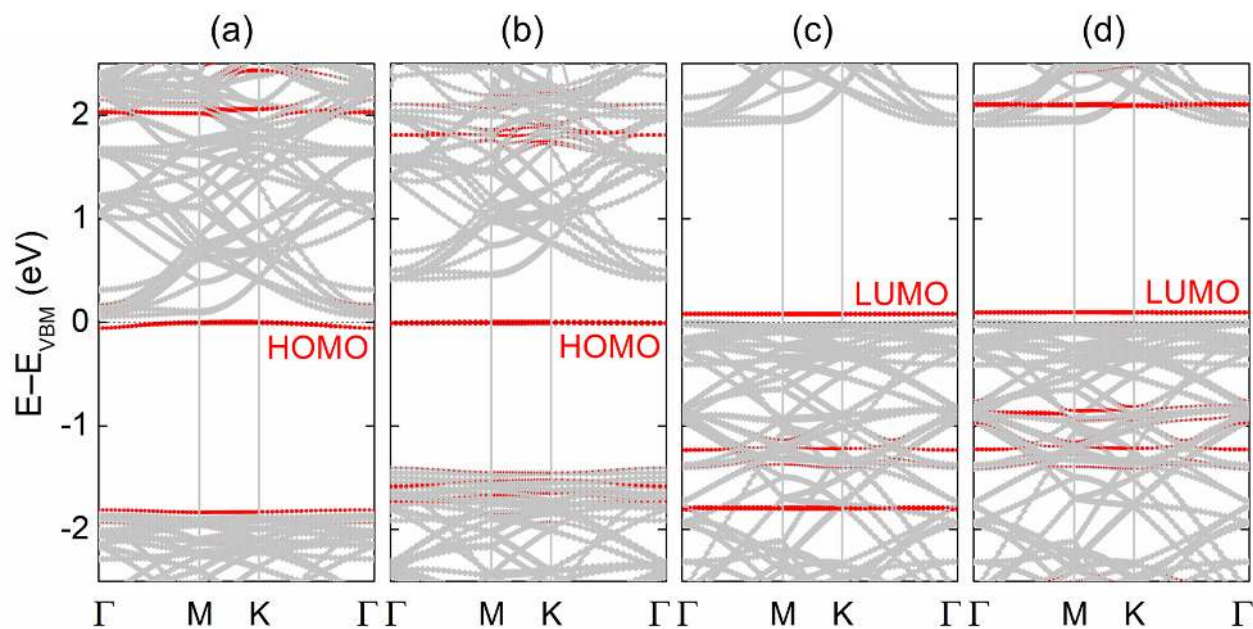
Figure 6. Projected band structures of (a) TTF–BlueP and (b) CCO–BlueP under an electric field of -0.5 V Å^{-1}, and of (c) F_4-TCNQ–BlueP and (d) F_6-TNAP–BlueP under an electric field of 0.5 V Å^{-1}. Red color highlights the contributions of the molecules.

(P atoms in the contact region), i.e. the TTF and CCO molecules act as electron donors. Bader analysis [73–75] shows that 0.11 and 0.04 electrons are transferred from the TTF and CCO molecules to BlueP, respectively. In the cases of F_4-TCNQ–BlueP and F_6-TNAP–BlueP (figures 3(c) and (d)) electrons are transferred from BlueP to the lowest unoccupied molecular orbital (LUMO), i.e. the F_4-TCNQ and F_6-TNAP molecules act as electron acceptors. The transferred electrons are found mainly in the interlayer region between molecule and BlueP as well as on the cyano groups of the F_4-TCNQ and F_6-TNAP molecules. Large gray isosurfaces at P atoms near the cyano groups reflect strong interaction. Bader analysis [73–75] shows that 0.12 and 0.16 electrons are transferred from BlueP to the F_4-TCNQ and F_6-TNAP molecules, respectively. The electron transfer from/to the TTF, CCO, F_4-TCNQ, and F_6-TNAP molecules leads to a carrier concentration of 3.3×10^{12}, 1.2×10^{12}, 3.6×10^{12}, and 4.8×10^{12} cm^{-2} in BlueP.

Figure 4 shows a projected band structure of pristine BlueP in comparison to results for TTF–BlueP, CCO–BlueP, F_4-TCNQ–BlueP, and F_6-TNAP–BlueP. Pristine BlueP has an indirect bandgap of 1.94 eV (figure 4(a)), in agreement with the findings of previous investigations [2, 3]. The band structures of TTF–BlueP (figure 4(b)) and CCO–BlueP (figure 4(c)) resemble that of pristine BlueP. However, additional flat bands emerge at 0.27 and 0.97 eV, respectively, i.e. below the conduction band minimum (CBM) of BlueP, reflecting n-doping of the host material. The flat bands represent localized electronic states due to the HOMOs of TTF and CCO. The doping gap (between CBM and HOMO for n-dopants, between LUMO and VBM for p-dopants) of TTF–BlueP is significantly smaller than that of TTF–BlackP (0.73 eV) [56]. For F_4-TCNQ–BlueP (figure 4(d)) and F_6-TNAP–BlueP (figure 4(e)) the LUMOs of F_4-TCNQ- and F_6-TNAP appear at 0.39 and 0.45 eV, respectively, i.e. above the valence band maximum (VBM) of BlueP, reflecting p-doping of the host material.

The n-dopants TTF and CCO as well as the p-dopants F_4-TCNQ and F_6-TNAP induce a large doping gap in BlueP, which makes them to ineffective doping molecules. We next investigate whether an external perpendicular electric field can help to overcome this issue. The dependence of the doping gap and electron transfer on the applied electric field is shown in figure 5 (results after re-relaxing the atomic coordinates in the electric field, which, however, induces only minor structural changes). The strength of the electric field ranges from -0.5 to 0.5 V Å^{-1} with the positive direction oriented from the molecule to BlueP, see the insets of figure 5. We note that the change in bandgap of pristine BlueP is negligible under such an electric field [3]. For TTF–BlueP and CCO–BlueP the electron transfer is reduced for increasing electric field, i.e., the HOMOs of the molecules shift toward the CBM of BlueP and the doping gaps increase monotonically. Under an electric field of -0.5 V Å^{-1} (figures 6(a) and (b)) the doping gaps are as small as 57 and 420 meV, respectively, reflecting good controllability. In particular, due to its shallow donor state, TTF–BlueP resembles a typical n-type semiconductor. It turns out that the charge transfer can be reversed by an electric field of 0.3 V Å^{-1}. For F_4-TCNQ–BlueP and F_6-TNAP–BlueP the
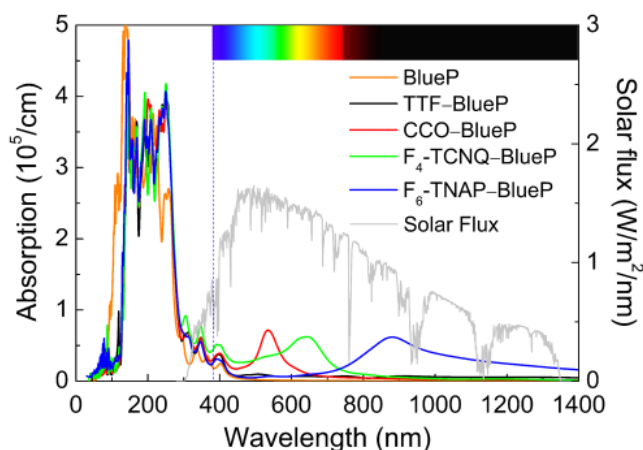

Figure 7. Absorption spectra of pristine BlueP, BlueP–TTF, BlueP–CCO, BlueP–T_4-TCNQ, and BlueP–T_6-TNAP as calculated with the HSE06 functional. The incident AM1.5g global standard spectrum is shown for comparison.

electron transfer grows for increasing electric field, i.e. the LUMOs of the molecules shift toward the VBM of BlueP and the doping gaps decrease monotonically. Under an electric field of 0.5 V Å^{-1} (figures 6(c) and (d)) the doping gaps are as small as 79 and 94 meV, respectively, indicating that shallow acceptor states are formed in both F_4-TCNQ–BlueP and F_6-TNAP–BlueP, resembling typical p-type semiconductors. We note that the HSE06 functional enhances the doping gaps, while maintaining the general trends described above.

In addition to enhancing the effectiveness of doping, applying an electric field also supports the charge carrier injection and therefore can be beneficial for the device performance. More specifically, according to figure 5, 0.44 electrons are transferred from TTF to BlueP, which leads to an n-type carrier concentration of 1.31×10^{13} cm^{-2} in BlueP. Transfer of 0.41 and 0.46 electrons from BlueP to F_4-TCNQ and F_6-TNAP, respectively, leads to p-type carrier concentrations of 1.22×10^{13} and 1.37×10^{13} cm^{-2} in BlueP.

Absorption spectra are shown in figure 7 together with the incident AM1.5g global standard spectrum. Pristine BlueP does not exhibit strong optical absorption in the visible region and, therefore, is not a good photovoltaic material. Similar results are obtained for TTF–BlueP. On the other hand, CCO–BlueP shows a pronounced absorption peak (intensity 7.2×10^4 cm^{-1}) in the visible region centered at 534 nm. For T_4-TCNQ–BlueP we obtain more enhancement of the absorption in the visible region with a broader absorption peak (intensity 6.2×10^4 cm^{-1}) centered at 641 nm. Finally, T_6-TNAP–BlueP realizes a very broad absorption peak (intensity 6.2×10^4 cm^{-1}) centered at 877 nm. Apart from these additional absorption peaks, which are mainly due to molecular transitions, we observe for all doped materials a redshift of the absorption spectrum with respect to pristine BlueP, which enlarges the overlap with the incident solar flux and thus further enhances their ability to absorb sun light. To quantify the performance of the materials under investigation, we calculate $\eta = \int_0^{+\infty} a(\lambda) S(\lambda) d\lambda$, where λ is the wavelength, $a(\lambda)$ is the absorption spectrum, and $S(\lambda)$ is the incident AM 1.5g global standard spectrum. We obtain for TTF–BlueP,

CCO–BlueP, F$_4$-TCNQ–BlueP, and F$_6$-TNAP–BlueP values of 10.6, 37.2, 24.1, and 28.8 W cm^{-3}, respectively. In particular, both CCO–BlueP and F$_6$-TNAP–BlueP therefore turn out to be superior to T$_4$-TCNQ–Arsenene (28.0 W cm^{-3}) [76].

Conclusions

Our investigation of molecular doping of BlueP, based on first-principles calculations, shows that TTF and CCO molecules act as electron donors and lead to n-doping of BlueP while F$_4$-TCNQ and F$_6$-TNAP molecules act as electron acceptors and lead to p-doping of BlueP. The amount of electron transfer, which determines the carrier dynamics and thus the device performance, has been quantified. It turns out that an external perpendicular electric field shifts the HOMO of TTF closer to the CBM of BlueP, resulting in a shallow donor state and effective n-doping of BlueP. Similarly, the LUMOs of F$_4$-TCNQ and F$_6$-TNAP can be shifted closer to the VBM of BlueP, resulting in shallow acceptor states and effective p-doping of BlueP. The application of an electric field also enhances the charge transfer and thus the charge carrier injection into BlueP. CCO, F$_4$-TCNQ, and F$_6$-TNAP molecules induce redshifts of the absorption spectrum of BlueP and enhance the absorption in the visible and infrared regions, which is beneficial for solar energy harvesting. Due to a lack of experimental studies, our results provide important insights into the electronic and optical properties achievable by molecular doping of BlueP. They offer guidelines for the design of electronic, optoelectronic, and photovoltaic devices.

Acknowledgment

Supporting information

Structural properties of TTF, CCO, F$_4$-TCNQ, and F$_6$-TNAP. Studied adsorption configurations of TTF, CCO, F$_4$-TCNQ, and F$_6$-TNAP molecules on BlueP.

Notes

The authors declare no competing financial interest.

ORCID iDs

Minglei Sun ⬤ https://orcid.org/0000-0001-5105-0065

Wencheng Tang ⬤ https://orcid.org/0000-0002-5113-5533
Song Li ⬤ https://orcid.org/0000-0002-8297-5199
Jyh-Pin Chou ⬤ https://orcid.org/0000-0001-8336-6793
Alice Hu ⬤ https://orcid.org/0000-0002-0883-315X
Udo Schwingenschlögl ⬤ https://orcid.org/0000-0003-4179-7231

References

[1] Zhu Z and Tománek D 2014 Semiconducting layered blue phosphorus: a computational study *Phys. Rev. Lett.* **112** 176802

[2] Montes E and Schwingenschlögl U 2016 Nanotubes based on monolayer blue phosphorus *Phys. Rev.* B **94** 035412

[3] Ghosh B, Nahas S, Bhowmick S and Agarwal A 2015 Electric field induced gap modification in ultrathin blue phosphorus *Phys. Rev.* B **91** 115433

[4] Mogulkoc Y, Modarresi M, Mogulkoc A and Ciftci Y O 2016 Electronic and optical properties of bilayer blue phosphorus *Comput. Mater. Sci.* **124** 23–9

[5] Pontes R B, Miwa R H, da Silva A J R, Fazzio A and Padilha J E 2018 Layer-dependent band alignment of few layers of blue phosphorus and their Van Der Waals heterostructures with graphene *Phys. Rev.* B **97** 235419

[6] Zhu L, Wang S-S, Guan S, Liu Y, Zhang T, Chen G and Yang S A 2016 Blue phosphorene oxide: strain-tunable quantum phase transitions and novel 2D emergent fermions *Nano Lett.* **16** 6548–54

[7] Yang G, Xu Z, Liu Z, Jin S, Zhang H and Ding Z 2017 Strain- and fluorination-induced quantum spin Hall insulators in blue phosphorene: a first-principles study *J. Phys. Chem.* C **121** 12945–52

[8] Sun M, Wang S, Yu J and Tang W 2017 Hydrogenated and halogenated blue phosphorene as dirac materials: a first principles study *Appl. Surf. Sci.* **392** 46–50

[9] Sun M, Tang W, Ren Q, Wang S-K, Yu J and Du Y 2015 A first-principles study of light non-metallic atom substituted blue phosphorene *Appl. Surf. Sci.* **356** 110–14

[10] Sun M, Hao Y, Ren Q, Zhao Y, Du Y and Tang W 2016 Tuning electronic and magnetic properties of blue phosphorene by boping Al, Si, As and Sb atom: a DFT calculation *Solid State Commun.* **242** 36–40

[11] Zhang W X, Zhao J W, He W H, Luan L J and He C 2017 Enhanced hydrophilic and conductive properties of blue phosphorene doped with Si atom *Chem. Phys. Lett.* **675** 20–6

[12] Sun M, Chou J-P, Yu J and Tang W 2017 Electronic properties of blue phosphorene/graphene and blue phosphorene/graphene-like gallium nitride heterostructures *Phys. Chem. Chem. Phys.* **19** 17324–30

[13] Mogulkoc Y, Modarresi M, Mogulkoc A and Alkan B 2018 Electronic and optical properties of boron phosphide/blue phosphorus heterostructures *Phys. Chem. Chem. Phys.* **20** 12053–60

[14] Kaewmaraya T, Srepusharawoot P, Hussian T and Amornkitbamrung V 2018 Electronic properties of h-BCN/blue phosphorene Van Der Waals heterostructures *ChemPhysChem* **19** 612–8

[15] Xiao J, Long M, Zhang X, Ouyang J, Xu H and Gao Y 2015 Theoretical predictions on the electronic structure and charge carrier mobility in 2D phosphorus sheets *Sci. Rep.* **5** 9961

[16] Cem S and Hâldun S 2016 Promising thermoelectric properties of phosphorenes *Nanotechnology* **27** 355705

[17] Li J *et al* 2017 Electrical contacts in monolayer blue phosphorene devices *Nano Res.* **11** 1834–49

[18] Montes E and Schwingenschlögl U 2017 Superior selectivity and sensitivity of blue phosphorus nanotubes in gas sensing applications *J. Mater. Chem.* C **5** 5365–71

[19] Safari F, Moradinasab M, Fathipour M and Kosina H 2018 Adsorption of the NH_3, NO, NO_2, CO_2, and CO gas molecules on blue phosphorene: a first-principles study *Appl. Surf. Sci.* **464** 153–61

[20] Bao J *et al* 2018 Hexagonal boron nitride/blue phosphorene heterostructure as a promising anode material for Li/Na-ion batteries *J. Phys. Chem.* C **122** 23329–35

[21] Li Q, Yang J and Zhang L 2018 Theoretical prediction of blue phosphorene/borophene heterostructure as a promising anode material for lithium-ion batteries *J. Phys. Chem.* C **122** 18294–303

[22] Ju L, Dai Y, Wei W, Liang Y and Huang B 2018 Potential of one-dimensional blue phosphorene nanotubes as a water splitting photocatalyst *J. Mater. Chem.* A **6** 21087–97

[23] Wang B-J, Li X-H, Zhao R, Cai X-L, Yu W-Y, Li W-B, Liu Z-S, Zhang L-W and Ke S-H 2018 Electronic structures and enhanced photocatalytic properties of blue phosphorene/BSe Van Der Waals heterostructures *J. Mater. Chem.* A **6** 8923–9

[24] Wang B-J, Li X-H, Cai X-L, Yu W-Y, Zhang L-W, Zhao R-Q and Ke S-H 2018 Blue phosphorus/Mg(OH)$_2$ Van Der Waals heterostructures as promising visible-light photocatalysts for water splitting *J. Phys. Chem.* C **122** 7075–80

[25] Zhang J L *et al* 2016 Epitaxial growth of single layer blue phosphorus: a new phase of two-dimensional phosphorus *Nano Lett.* **16** 4903–8

[26] Zhang W, Enriquez H, Tong Y, Bendounan A, Kara A, Seitsonen A P, Mayne A J, Dujardin G and Oughaddou H 2018 Epitaxial synthesis of blue phosphorene *Small* 1804066

[27] Zhuang J *et al* 2018 Band gap modulated by electronic superlattice in blue phosphorene *ACS Nano* **12** 5059–65

[28] Zeng J, Cui P and Zhang Z 2017 Half layer by half layer growth of a blue phosphorene monolayer on a GaN (0 0 1) substrate *Phys. Rev. Lett.* **118** 046101

[29] Dong X, Shi Y, Zhao Y, Chen D, Ye J, Yao Y, Gao F, Ni Z, Yu T and Shen Z 2009 Symmetry breaking of graphene monolayers by molecular decoration *Phys. Rev. Lett.* **102** 135501

[30] Lu Y H, Chen W, Feng Y P and He P M 2009 Tuning the electronic structure of graphene by an organic molecule *J. Phys. Chem.* B **113** 2–5

[31] Yong-Hui Z, Kai-Ge Z, Ke-Feng X, Jing Z, Hao-Li Z and Yong P 2010 Tuning the electronic structure and transport properties of graphene by noncovalent functionalization: effects of organic donor, acceptor and metal atoms *Nanotechnology* **21** 065201

[32] Zhang Z, Huang H, Yang X and Zang L 2011 Tailoring electronic properties of graphene by π–π stacking with aromatic molecules *J. Phys. Chem. Lett.* **2** 2897–905

[33] Miao X, Tongay S, Petterson M K, Berke K, Rinzler A G, Appleton B R and Hebard A F 2012 High efficiency graphene solar cells by chemical doping *Nano Lett.* **12** 2745–50

[34] Hong G, Wu Q-H, Ren J, Wang C, Zhang W and Lee S-T 2013 Recent progress in organic molecule/graphene interfaces *Nano Today* **8** 388–402

[35] Lazar P, Karlický F, Jurečka P, Kocman M, Otyepková E, Šafářová K and Otyepka M 2013 Adsorption of small organic molecules on graphene *J. Am. Chem. Soc.* **135** 6372–7

[36] Samuels A J and Carey J D 2013 Molecular doping and band-gap opening of bilayer graphene *ACS Nano* **7** 2790–9

[37] Chen L, Wang L, Shuai Z and Beljonne D 2013 Energy level alignment and charge carrier mobility in noncovalently functionalized graphene *J. Phys. Chem. Lett.* **4** 2158–65

[38] Hu T and Gerber I C 2013 Theoretical study of the interaction of electron donor and acceptor molecules with graphene *J. Phys. Chem.* C **117** 2411–20

[39] Wang T H, Zhu Y F and Jiang Q 2013 Bandgap opening of bilayer graphene by dual doping from organic molecule and substrate *J. Phys. Chem.* C **117** 12873–81

[40] de Oliveira I S S and Miwa R H 2015 Organic molecules deposited on graphene: a computational investigation of self-assembly and electronic structure *J. Chem. Phys.* **142** 044301

[41] Néel N, Lattelais M, Bocquet M-L and Kröger J 2016 Depopulation of single-phthalocyanine molecular orbitals upon pyrrolic-hydrogen abstraction on graphene *ACS Nano* **10** 2010–6

[42] Solís-Fernández P, Okada S, Sato T, Tsuji M and Ago H 2016 Gate-tunable dirac point of molecular doped graphene *ACS Nano* **10** 2930–9

[43] Kumar A, Banerjee K, Dvorak M, Schulz F, Harju A, Rinke P and Liljeroth P 2017 Charge-transfer-driven nonplanar adsorption of F_4TCNQ molecules on epitaxial graphene *ACS Nano* **11** 4960–8

[44] Pham V D *et al* 2019 Selective control of molecule charge state on graphene using tip-induced electric field and nitrogen doping *NPJ 2D Mater. Appl.* **3** 5

[45] Mouri S, Miyauchi Y and Matsuda K 2013 Tunable photoluminescence of monolayer MoS_2 via chemical doping *Nano Lett.* **13** 5944–8

[46] Perkins F K, Friedman A L, Cobas E, Campbell P M, Jernigan G G and Jonker B T 2013 Chemical vapor sensing with monolayer MoS_2 *Nano Lett.* **13** 668–73

[47] Dhakal K P, Duong D L, Lee J, Nam H, Kim M, Kan M, Lee Y H and Kim J 2014 Confocal absorption spectral imaging of MoS_2: optical transitions depending on the atomic thickness of intrinsic and chemically doped MoS_2 *Nanoscale* **6** 13028–35

[48] Li J *et al* 2014 Tuning the optical emission of MoS_2 nanosheets using proximal photoswitchable azobenzene molecules *Appl. Phys. Lett.* **105** 241116

[49] Kiriya D, Tosun M, Zhao P, Kang J S and Javey A 2014 Air-stable surface charge transfer doping of MoS_2 by benzyl viologen *J. Am. Chem. Soc.* **136** 7853–6

[50] Jing Y, Tan X, Zhou Z and Shen P 2014 Tuning electronic and optical properties of MoS_2 monolayer via molecular charge transfer *J. Mater. Chem.* A **2** 16892–7

[51] Kang D-H, Kim M-S, Shim J, Jeon J, Park H-Y, Jung W-S, Yu H-Y, Pang C-H, Lee S and Park J-H 2015 High-performance transition metal dichalcogenide photodetectors enhanced by self-assembled monolayer doping *Adv. Funct. Mater.* **25** 4219–27

[52] Su W, Dou H, Huo D, Dai N and Yang L 2015 Enhancing photoluminescence of trion in single-layer MoS_2 using p-type aromatic molecules *Chem. Phys. Lett.* **635** 40–4

[53] Tarasov A, Zhang S, Tsai M-Y, Campbell P M, Graham S, Barlow S, Marder S R and Vogel E M 2015 Controlled doping of large-area trilayer MoS_2 with molecular reductants and oxidants *Adv. Mater.* **27** 1175–81

[54] Cai Y, Zhou H, Zhang G and Zhang Y-W 2016 Modulating carrier density and transport properties of MoS_2 by organic molecular doping and defect engineering *Chem. Mater.* **28** 8611–21

[55] He Y, Xia F, Shao Z, Zhao J and Jie J 2015 Surface charge transfer doping of monolayer phosphorene via molecular adsorption *J. Phys. Chem. Lett.* **6** 4701–10

[56] Zhang R, Li B and Yang J 2015 A first-principles study on electron donor and acceptor molecules adsorbed on phosphorene *J. Phys. Chem.* C **119** 2871–8

[57] Yu Z G, Zhang Y-W and Yakobson B I 2016 Phosphorene-based nanogenerator powered by cyclic molecular doping *Nano Energy* **23** 34–9

[58] Yu X, Zhang S, Zeng H and Wang Q J 2016 Lateral black phosphorene p-n junctions formed via chemical doping for high performance near-infrared photodetector *Nano Energy* **25** 34–41

[59] Wang C, Niu D, Liu B, Wang S, Wei X, Liu Y, Xie H and Gao Y 2017 Charge transfer at the PTCDA/black phosphorus interface *J. Phys. Chem.* C **121** 18084–94

[60] Gao N, Zhu Y F and Jiang Q 2017 Formation of arsenene p-n junctions via organic molecular adsorption *J. Mater. Chem.* C **5** 7283–90

[61] Deobrat S, Sanjeev K G, Yogesh S and Satyaprakash S 2017 Modulating the electronic and optical properties of monolayer arsenene phases by organic molecular doping *Nanotechnology* **28** 495202

[62] Abellán G *et al* 2017 Noncovalent functionalization and charge transfer in antimonene *Angew. Chem., Int. Ed. Engl.* **129** 14581–6

[63] Gleiter R, Schmidt E, Cowan D O and Ferraris J P 1973 The electronic structure of tetrathiofulvalene *J. Electron. Spectrosc.* **2** 207–10

[64] Baumann H, Bünzli J-C and Oth J F M 1982 The photoelectron spectrum of [18]annulene *Helv. Chim. Acta* **65** 582–6

[65] Gao W and Kahn A 2001 Controlled p-doping of zinc phthalocyanine by coevaporation with tetrafluorotetracyanoquinodimethane: a direct and inverse photoemission study *Appl. Phys. Lett.* **79** 4040–2

[66] Koech P K, Padmaperuma A B, Wang L, Swensen J S, Polikarpov E, Darsell J T, Rainbolt J E and Gaspar D J 2010 Synthesis and application of 1,3,4,5,7,8-hexafluorotetracyanonaphthoquinodimethane (F6-TNAP): a conductivity dopant for organic light-emitting devices *Chem. Mater.* **22** 3926–32

[67] Kresse G and Joubert D 1999 From ultrasoft pseudopotentials to the projector augmented-wave method *Phys. Rev.* B **59** 1758–75

[68] Grimme S, Antony J, Ehrlich S and Krieg H 2010 A consistent and accurate *ab initio* parametrization of density functional dispersion correction (DFT-D) for the 94 elements H-Pu *J. Chem. Phys.* **132** 154104

[69] Klimeš J, David R B and Angelos M 2009 Chemical accuracy for the Van Der Waals density functional *J. Phys.: Condens. Matter* **22** 022201

[70] Han N, Gao N and Zhao J 2007 Initial growth mechanism of blue phosphorene on Au(1 1 1) surface *J. Phys. Chem.* C **121** 17893–9

[71] Heyd J, Scuseria G E and Ernzerhof M 2003 Hybrid functionals based on a screened coulomb potential *J. Chem. Phys.* **118** 8207–15

[72] Gajdoš M, Hummer K, Kresse G, Furthmüller J and Bechstedt F 2006 Linear optical properties in the projector-augmented wave methodology *Phys. Rev.* B **73** 045112

[73] Henkelman G, Arnaldsson A and Jónsson H 2006 A fast and robust algorithm for bader decomposition of charge density *Comput. Mater. Sci.* **36** 354–60

[74] Sanville E, Kenny S D, Smith R and Henkelman G 2007 Improved grid-based algorithm for bader charge allocation *J. Comput. Chem.* **28** 899–908

[75] Tang W, Sanville E and Henkelman G 2009 A grid-based bader analysis algorithm without lattice bias *J. Phys.: Condens. Matter* **21** 084204

[76] Sun M, Chou J-P, Gao J, Cheng Y, Hu A, Tang W and Zhang G 2018 Exceptional optical absorption of buckled arsenene covering a broad spectral range by molecular doping *ACS Omega* **3** 8514–20